

---

## Electrons in the Periodic Potential of a Crystal

The discussion of the properties of metals in the previous chapter was based on a free-electron model (or rather: a gas of neutral fermionic particles) in an empty box. The classical Drude model and the quantum mechanical Sommerfeld model (based on the Fermi–Dirac statistics) were introduced, and it was shown that a suitable choice of certain parameters leads to a good description of several properties of simple metals. We have to specify which electrons of the atoms remain bound in the ion core and which can be considered free (and hence can participate in conduction in the solid state). The number of conduction electrons is an important parameter even in the Drude model. In much the same way, in the Sommerfeld model various properties of metals are determined through the Fermi energy, by the number of conduction electrons per atom. Since core electrons are ignored, these models obviously cannot account for the electrical properties of ionically or covalently bonded materials, in which electrons are fairly well localized to the ions and covalent bonds. Therefore not even the quantum mechanical model can explain the existence of insulators and semiconductors. However, the conduction electrons are not perfectly free even in metals, since they move through the regular crystalline array of ions, thus their motion is determined by the periodic crystal potential. To resolve these difficulties and contradictions, the behavior of the electrons has to be studied in the presence of the atoms (ions) that make up the crystal lattice.

As a first approximation, we shall consider ions to be fixed at the lattice points, and ignore their vibrations, the phonons. The justification of this approximation and the influence of the motion of ions on the electrons will be discussed in Chapter 23. In the present chapter we shall lump the effects of ions into a local static potential  $U_{\text{ion}}(\mathbf{r})$  that can be taken as the sum of the individual atomic potentials  $v_a(\mathbf{r} - \mathbf{R}_m)$  of periodically spaced ions.

Taking into account the influence of other electrons is much more difficult. Only by employing the methods of the many-body problem can electron–electron interactions be treated more or less precisely. We shall delve into this complex subject in Volume 3. Below we shall assume that electrons feel the

influence of the others only in an average sense, through the averaged potential  $U_{\text{el}}(\mathbf{r})$  that also possesses the periodicity of the lattice. In this chapter we shall examine how the electronic states can be described in ideal crystals and present some general features of the energy spectrum without any assumptions about the actual form of this periodic potential. At the end of the chapter we shall briefly discuss what happens to the electrons if the structure is not perfectly crystalline. The methods to determine energy eigenvalues for specific periodic potentials will be discussed in the next chapters.

## 17.1 Band Structure of Electronic States

In this section we shall first introduce the Bloch functions – that is, the Bloch form of electron wavefunctions obtained in the presence of a periodic potential using the Bloch theorem (formulated in full generality in Chapter 6), and then determine some general properties of the electron spectrum.

### 17.1.1 Bloch States

As mentioned in the introductory part, we shall assume that electrons feel the presence of ions and other electrons only through the spin-independent lattice-periodic potentials  $U_{\text{ion}}(\mathbf{r})$  and  $U_{\text{el}}(\mathbf{r})$ . Therefore the same one-particle potential,

$$U(\mathbf{r}) = U_{\text{ion}}(\mathbf{r}) + U_{\text{el}}(\mathbf{r}) \quad (17.1.1)$$

acts on each electron. Using this averaged potential, the Hamiltonian of a system of  $N_e$  electrons is

$$\mathcal{H}_{\text{el}} = -\frac{\hbar^2}{2m_e} \sum_{i=1}^{N_e} \frac{\partial^2}{\partial \mathbf{r}_i^2} + \sum_{i=1}^{N_e} U(\mathbf{r}_i). \quad (17.1.2)$$

This Hamiltonian is the sum of independent one-particle Hamiltonians. Therefore when the solutions of the one-particle Schrödinger equation

$$\mathcal{H}(\mathbf{r})\psi_i(\mathbf{r}) \equiv \left[ -\frac{\hbar^2}{2m_e} \nabla^2 + U(\mathbf{r}) \right] \psi_i(\mathbf{r}) = \varepsilon_i \psi_i(\mathbf{r}) \quad (17.1.3)$$

are known, the total wavefunction  $\Psi$  of the electron system can be written as the Slater determinant of the wavefunctions of occupied one-particle states, thereby satisfying the requirement that the total wavefunction should be completely antisymmetric. Since the potential is spin-independent, as the spin-orbit interaction is ignored here, only the spatial parts of the wavefunctions are considered. Nevertheless, when writing down the Slater determinant, the requirement of complete antisymmetry applies to the spin variables as well:

$$\Psi = \frac{1}{\sqrt{N_e!}} \begin{vmatrix} \psi_{i_1, \sigma_1}(\mathbf{r}_1, s_1) & \psi_{i_1, \sigma_1}(\mathbf{r}_2, s_2) & \dots & \psi_{i_1, \sigma_1}(\mathbf{r}_{N_e}, s_{N_e}) \\ \psi_{i_2, \sigma_2}(\mathbf{r}_1, s_1) & \psi_{i_2, \sigma_2}(\mathbf{r}_2, s_2) & \dots & \psi_{i_2, \sigma_2}(\mathbf{r}_{N_e}, s_{N_e}) \\ \vdots & \vdots & \ddots & \vdots \\ \psi_{i_{N_e}, \sigma_{N_e}}(\mathbf{r}_1, s_1) & \psi_{i_{N_e}, \sigma_{N_e}}(\mathbf{r}_2, s_2) & \dots & \psi_{i_{N_e}, \sigma_{N_e}}(\mathbf{r}_{N_e}, s_{N_e}) \end{vmatrix}. \quad (17.1.4)$$

Because of the periodicity of the crystal structure, the potential  $U(\mathbf{r})$  satisfies the condition

$$U(\mathbf{r} + \mathbf{t}_m) = U(\mathbf{r}), \quad (17.1.5)$$

where  $\mathbf{t}_m$  is an arbitrary translation vector of the crystal lattice. Along with the potential, the full Hamiltonian is also lattice periodic, and satisfies (6.2.1). In accordance with Bloch's theorem, solutions must satisfy the condition

$$\boxed{\psi_{\mathbf{k}}(\mathbf{r} + \mathbf{t}_m) = e^{i\mathbf{k} \cdot \mathbf{t}_m} \psi_{\mathbf{k}}(\mathbf{r})} \quad (17.1.6)$$

given in (6.2.5), where the vector  $\mathbf{k}$  can take discrete values allowed by the periodic boundary condition.

The Bloch condition on the wavefunction can be formulated in another way by separating the phase factor  $e^{i\mathbf{k} \cdot \mathbf{r}}$  off the wavefunction, and by introducing the function  $u_{\mathbf{k}}(\mathbf{r})$  through the definition

$$\boxed{\psi_{\mathbf{k}}(\mathbf{r}) = e^{i\mathbf{k} \cdot \mathbf{r}} u_{\mathbf{k}}(\mathbf{r})}. \quad (17.1.7)$$

It follows directly from (17.1.6) that

$$\psi_{\mathbf{k}}(\mathbf{r} + \mathbf{t}_m) = e^{i\mathbf{k} \cdot \mathbf{t}_m} e^{i\mathbf{k} \cdot \mathbf{r}} u_{\mathbf{k}}(\mathbf{r}). \quad (17.1.8)$$

On the other hand, if the wavefunction given in (17.1.7) is taken at the translated position  $\mathbf{r} + \mathbf{t}_m$ , we find

$$\psi_{\mathbf{k}}(\mathbf{r} + \mathbf{t}_m) = e^{i\mathbf{k} \cdot (\mathbf{r} + \mathbf{t}_m)} u_{\mathbf{k}}(\mathbf{r} + \mathbf{t}_m). \quad (17.1.9)$$

Comparison of the two formulas gives

$$\boxed{u_{\mathbf{k}}(\mathbf{r} + \mathbf{t}_m) = u_{\mathbf{k}}(\mathbf{r})}, \quad (17.1.10)$$

that is, the function  $u_{\mathbf{k}}(\mathbf{r})$  obtained by the separation of the phase factor is periodic with the periodicity of the lattice. Bloch's theorem is therefore equivalent to the statement that *the eigenfunctions of a lattice-periodic Hamiltonian can be written in the form (17.1.7), where the  $u_{\mathbf{k}}(\mathbf{r})$  are lattice-periodic functions*. Wavefunctions of this form are called Bloch functions.<sup>1</sup> Such a function  $u_{\mathbf{k}}(\mathbf{r})$  and the real part of the corresponding Bloch function are shown in Fig. 17.1.

<sup>1</sup> Sometimes the lattice-periodic functions  $u_{\mathbf{k}}(\mathbf{r})$  are called Bloch functions in the literature.

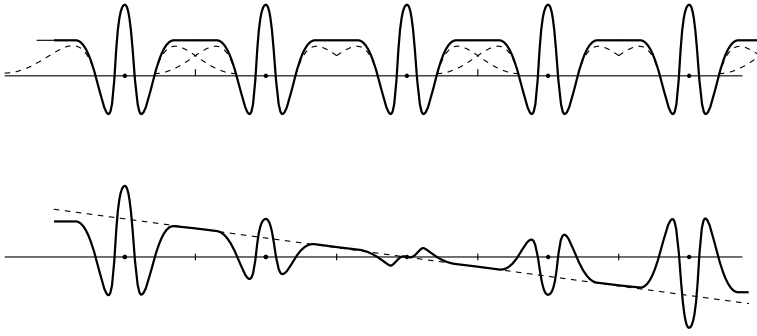


**Fig. 17.1.** A lattice-periodic function  $u(x)$  and the real part of the corresponding Bloch function

In the absence of a periodic potential the wavefunction is a plane wave  $e^{i\mathbf{k}\cdot\mathbf{r}}/\sqrt{V}$ . The function  $u_{\mathbf{k}}(\mathbf{r})$  describes the deformation of the wavefunction relative to the plane wave. This deformation is identical for each primitive cell of the crystal. It would, therefore, be more natural to define the Bloch function as

$$\boxed{\psi_{\mathbf{k}}(\mathbf{r}) = \frac{1}{\sqrt{V}} e^{i\mathbf{k}\cdot\mathbf{r}} u_{\mathbf{k}}(\mathbf{r})} \quad (17.1.11)$$

instead of (17.1.7). Nonetheless we shall often drop the factor  $1/\sqrt{V}$  wherever this does not cause confusion.

The form (17.1.7) of the Bloch function immediately confirms our previous remark that  $\hbar\mathbf{k}$  is not the momentum of the Bloch state. The momentum operator transforms wavefunctions that satisfy the Bloch theorem into

$$\frac{\hbar}{i} \nabla \psi_{\mathbf{k}}(\mathbf{r}) = \frac{\hbar}{i} \nabla (e^{i\mathbf{k}\cdot\mathbf{r}} u_{\mathbf{k}}(\mathbf{r})) = \hbar\mathbf{k} \psi_{\mathbf{k}}(\mathbf{r}) + e^{i\mathbf{k}\cdot\mathbf{r}} \frac{\hbar}{i} \nabla u_{\mathbf{k}}(\mathbf{r}) \quad (17.1.12)$$

indicating that  $\psi_{\mathbf{k}}(\mathbf{r})$  is not an eigenstate of the momentum operator.

### 17.1.2 Energy Levels of Bloch States

Substituting the one-particle wavefunction (17.1.7) into the Schrödinger equation (17.1.3),

$$\left[ -\frac{\hbar^2}{2m_e} \nabla^2 + U(\mathbf{r}) \right] e^{i\mathbf{k}\cdot\mathbf{r}} u_{\mathbf{k}}(\mathbf{r}) = \varepsilon_{\mathbf{k}} e^{i\mathbf{k}\cdot\mathbf{r}} u_{\mathbf{k}}(\mathbf{r}). \quad (17.1.13)$$

Differentiating the exponential factor and separating  $e^{i\mathbf{k}\cdot\mathbf{r}}$  on both sides, the function  $u_{\mathbf{k}}(\mathbf{r})$  satisfies the equation

$$\left[ \frac{\hbar^2 \mathbf{k}^2}{2m_e} - \frac{i\hbar^2}{m_e} \mathbf{k} \cdot \nabla - \frac{\hbar^2}{2m_e} \nabla^2 + U(\mathbf{r}) \right] u_{\mathbf{k}}(\mathbf{r}) = \varepsilon_{\mathbf{k}} u_{\mathbf{k}}(\mathbf{r}). \quad (17.1.14)$$

We shall also use the equivalent form

$$\left[ \frac{1}{2m_e} \left( \frac{\hbar}{i} \nabla + \hbar \mathbf{k} \right)^2 + U(\mathbf{r}) \right] u_{\mathbf{k}}(\mathbf{r}) = \varepsilon_{\mathbf{k}} u_{\mathbf{k}}(\mathbf{r}). \quad (17.1.15)$$

By introducing the notation

$$\mathcal{H}_{\mathbf{k}} = \frac{1}{2m_e} \left( \frac{\hbar}{i} \nabla + \hbar \mathbf{k} \right)^2 + U(\mathbf{r}), \quad (17.1.16)$$

(17.1.15) can be considered as an eigenvalue equation for the function  $u_{\mathbf{k}}(\mathbf{r})$ :

$$\mathcal{H}_{\mathbf{k}} u_{\mathbf{k}}(\mathbf{r}) = \varepsilon_{\mathbf{k}} u_{\mathbf{k}}(\mathbf{r}). \quad (17.1.17)$$

Since  $u_{\mathbf{k}}(\mathbf{r})$  is lattice periodic, it is sufficient to solve this equation for a single primitive cell of the crystal, with periodic boundary conditions, however the solutions have to be found for all possible values of  $\mathbf{k}$ .

The eigenvalue problem has infinitely many solutions for each  $\mathbf{k}$ . We shall label them by a second index,  $n$ . The eigenvalue equation to be solved is then

$$\left[ \frac{\hbar^2 \mathbf{k}^2}{2m_e} - \frac{i\hbar^2}{m_e} \mathbf{k} \cdot \nabla - \frac{\hbar^2}{2m_e} \nabla^2 + U(\mathbf{r}) \right] u_{n\mathbf{k}}(\mathbf{r}) = \varepsilon_{n\mathbf{k}} u_{n\mathbf{k}}(\mathbf{r}). \quad (17.1.18)$$

The Bloch functions  $\psi_{n\mathbf{k}}(\mathbf{r})$  form a complete orthonormal set:

$$\int \psi_{n\mathbf{k}}^*(\mathbf{r}) \psi_{n'\mathbf{k}'}(\mathbf{r}) d\mathbf{r} = \delta_{n,n'} \delta_{\mathbf{k},\mathbf{k}'}, \quad (17.1.19)$$

and

$$\sum_{n\mathbf{k}} \psi_{n\mathbf{k}}^*(\mathbf{r}) \psi_{n\mathbf{k}}(\mathbf{r}') = \delta(\mathbf{r} - \mathbf{r}'). \quad (17.1.20)$$

Figure 17.2 shows for each allowed value of  $\mathbf{k}$  the four lowest energy eigenvalues (obtained for an arbitrarily chosen potential) for chains of the same lattice constant  $a$  but different lengths  $L = Na$  subject to Born–von Kármán boundary conditions.

In short chains, where the Brillouin zone contains only a few allowed wave numbers  $k$ , the location of the energy levels seem to lack any order. When the number of atoms is increased, the allowed  $k$  values fill the region  $(-\pi/a, \pi/a)$  more densely, and the energy eigenvalues  $\varepsilon_{n\mathbf{k}}$  are arranged in such a way that in the  $N \rightarrow \infty$  limit they make up continuous curves that are similar to phonon dispersion curves. In finite but sufficiently long chains energy eigenvalues can be labeled in such a manner that for a given  $n$  the energies associated with adjacent  $k$  values are close – that is,  $\varepsilon_{n\mathbf{k}}$  can be approximated by a continuous function in  $k$ -space. If there are several states with close-by energies, one can impose the requirement that the continuous approximation of  $\varepsilon_{n\mathbf{k}}$  should also have a continuous derivative. The energies of the states associated with a particular  $n$  are then arranged into bands, which explains why the label  $n$  is called the band index. Similarly, band indices can be assigned to the levels of the electronic energy spectrum in three-dimensional crystals, too.

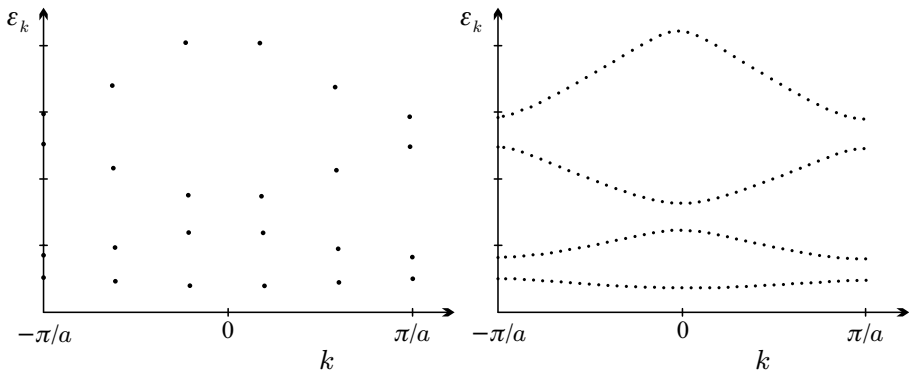


**Fig. 17.2.** The energy levels of electrons moving in the periodic potential of one-dimensional chains made up of 5 and 40 atoms

### 17.1.3 Eigenvalue Problem for Equivalent $\mathbf{k}$ Vectors

The  $\mathbf{k}$  vectors that characterize the behavior of the eigenstates of a lattice-periodic system under translations were defined in the cell spanned by the primitive vectors of the reciprocal lattice in Chapter 6. It was then shown that, as far as translational symmetries are concerned, an equivalent description is obtained when the vectors  $\mathbf{k}$  are replaced by vectors  $\mathbf{k}' = \mathbf{k} + \mathbf{G}$  that differ from them in a vector of the reciprocal lattice. Equivalence means that the same results are obtained for measurable quantities such as the energy spectrum or the spatial density of electrons. On the other hand, the wavefunction can receive an extra phase factor. We shall demonstrate these for the states given in terms of Bloch functions.

We shall first show that by replacing  $\mathbf{k}$  (defined in the primitive cell) by its equivalent  $\mathbf{k}' = \mathbf{k} + \mathbf{G}$  (defined in the Brillouin zone), the wavefunction of the state can be written in the Bloch form in terms of the new wave vector. To this end, we shall write the Bloch function

$$\psi_{n\mathbf{k}}(\mathbf{r}) = e^{i\mathbf{k}\cdot\mathbf{r}} u_{n\mathbf{k}}(\mathbf{r}) \quad (17.1.21)$$

as

$$\psi_{n\mathbf{k}}(\mathbf{r}) = e^{i(\mathbf{k}' - \mathbf{G})\cdot\mathbf{r}} u_{n\mathbf{k}}(\mathbf{r}) = e^{i\mathbf{k}'\cdot\mathbf{r}} u_{n\mathbf{k}'}(\mathbf{r}), \quad (17.1.22)$$

where

$$u_{n\mathbf{k}'}(\mathbf{r}) = u_{n,\mathbf{k}+\mathbf{G}}(\mathbf{r}) = e^{-i\mathbf{G}\cdot\mathbf{r}} u_{n\mathbf{k}}(\mathbf{r}). \quad (17.1.23)$$

It follows immediately from the lattice periodicity of  $u_{n\mathbf{k}}(\mathbf{r})$  and (5.2.20) that

$$u_{n\mathbf{k}'}(\mathbf{r} + \mathbf{t}_m) = u_{n\mathbf{k}'}(\mathbf{r}), \quad (17.1.24)$$

that is, this function is also lattice periodic. As the probability of finding the electron at  $\mathbf{r}$  is  $|u_{n\mathbf{k}}(\mathbf{r})|^2$ , and (17.1.23) implies  $|u_{n\mathbf{k}'}(\mathbf{r})|^2 = |u_{n\mathbf{k}}(\mathbf{r})|^2$ , the states associated with  $\mathbf{k}$  and  $\mathbf{k} + \mathbf{G}$  are equivalent in this sense.

It is worth noting that the Bloch function  $\psi_{n\mathbf{k}}(\mathbf{r})$  is periodic in reciprocal space and satisfies (17.1.6) in real space, while  $u_{n\mathbf{k}}(\mathbf{r})$  is periodic in real space and satisfies (17.1.23) in reciprocal space.

Let us now examine the eigenvalue problem of the states associated with the equivalent vectors  $\mathbf{k} + \mathbf{G}$ . From (17.1.18) we have

$$\left[ \frac{\hbar^2(\mathbf{k} + \mathbf{G})^2}{2m_e} - \frac{i\hbar^2}{m_e}(\mathbf{k} + \mathbf{G}) \cdot \nabla - \frac{\hbar^2}{2m_e} \nabla^2 + U(\mathbf{r}) \right] u_{n,\mathbf{k}+\mathbf{G}}(\mathbf{r}) = \varepsilon_{n,\mathbf{k}+\mathbf{G}} u_{n,\mathbf{k}+\mathbf{G}}(\mathbf{r}). \quad (17.1.25)$$

Expressing  $u_{n,\mathbf{k}+\mathbf{G}}(\mathbf{r})$  in terms of  $u_{n\mathbf{k}}(\mathbf{r})$  through (17.1.23), differentiation of the exponential factor leads to

$$\left[ \frac{\hbar^2 \mathbf{k}^2}{2m_e} - \frac{i\hbar^2}{m_e} \mathbf{k} \cdot \nabla - \frac{\hbar^2}{2m_e} \nabla^2 + U(\mathbf{r}) \right] u_{n\mathbf{k}}(\mathbf{r}) = \varepsilon_{n,\mathbf{k}+\mathbf{G}} u_{n\mathbf{k}}(\mathbf{r}). \quad (17.1.26)$$

Comparison with (17.1.18) gives

$$\varepsilon_{n,\mathbf{k}+\mathbf{G}} = \varepsilon_{n\mathbf{k}}, \quad (17.1.27)$$

that is, equivalent  $\mathbf{k}$  vectors are associated with the same energy.

#### 17.1.4 Role of the Spin–Orbit Interaction

Up to now electrons were assumed to feel a spin-independent potential, and thus energy eigenstates were independent of the spin orientation:  $\varepsilon_{n\mathbf{k}\uparrow} = \varepsilon_{n\mathbf{k}\downarrow}$ . In the absence of a magnetic field energies are therefore doubly degenerate. However, in the field of heavy ions, where relativistic effects cannot be ignored, spin–orbit coupling must also be considered. Using (3.1.30) – or more precisely its spin-dependent part, which gives the most important contribution –, the one-particle states have to be determined from the equation

$$\left[ -\frac{\hbar^2}{2m_e} \nabla^2 + U(\mathbf{r}) + \frac{\hbar^2}{4im_e^2 c^2} \boldsymbol{\sigma} \cdot ((\nabla U(\mathbf{r})) \times \nabla) \right] \psi_{n\mathbf{k}}(\mathbf{r}) = \varepsilon_{n\mathbf{k}} \psi_{n\mathbf{k}}(\mathbf{r}), \quad (17.1.28)$$

rather than (17.1.13). In this formula  $\psi_{n\mathbf{k}}(\mathbf{r})$  is a two-component spinor.

Writing the electron wavefunction in its Bloch form, the equation for  $u_{n\mathbf{k}}(\mathbf{r})$  reads

$$\left\{ \frac{1}{2m_e} \left( \frac{\hbar}{i} \nabla + \hbar \mathbf{k} \right)^2 + U(\mathbf{r}) + \frac{\hbar}{4m_e^2 c^2} \boldsymbol{\sigma} \cdot \left[ \nabla U(\mathbf{r}) \times \frac{\hbar}{i} \nabla \right] + \frac{\hbar^2}{4m_e^2 c^2} \mathbf{k} \cdot [\boldsymbol{\sigma} \times \nabla U(\mathbf{r})] \right\} u_{n\mathbf{k}}(\mathbf{r}) = \varepsilon_{n\mathbf{k}} u_{n\mathbf{k}}(\mathbf{r}). \quad (17.1.29)$$

As we shall see in connection with the band structure of semiconductors in Sec. 20.2, this interaction splits certain – otherwise degenerate – bands. If

the crystal does not possess inversion symmetry (which is the case for the sphalerite structure among others), the relation  $\varepsilon_{n,\mathbf{k},\alpha} = \varepsilon_{n,-\mathbf{k},\beta}$ , implied by time reversal and Kramers' theorem, continues to hold. This relation establishes that for each state there exists another one with the same energy but opposite wave vector and spin, while for a given  $\mathbf{k}$  the two spin states are of different energy. This is known as the *Dresselhaus splitting*.<sup>2</sup> On the other hand, when the crystal possesses inversion symmetry,  $u_{n,-\mathbf{k}}(\mathbf{r}) = u_{n,\mathbf{k}}(-\mathbf{r})$  and  $\varepsilon_{n,\mathbf{k},\alpha} = \varepsilon_{n,-\mathbf{k},\alpha}$ . Combined with time reversal,  $\varepsilon_{n,\mathbf{k},\alpha} = \varepsilon_{n,\mathbf{k},\beta}$ , which shows that spin degeneracy is preserved.

## 17.2 Representation of the Band Structure

A complete knowledge of the band structure requires the solution of the eigenvalue problem for each vector  $\mathbf{k}$  of the primitive cell of the reciprocal lattice (or the Brillouin zone) – that is, the relation between energy and wave vector has to be computed for each band. Since the problem is usually solved numerically, this would require the specification of an excessively large amount of data. Much like for the determination of the phonon spectrum, calculations are usually performed only for some special, high-symmetry directions of the Brillouin zone, and the dispersion curves of Bloch electrons are also displayed only along these directions. For materials that crystallize in fcc structure (whose Brillouin zone is shown in Fig. 7.11), the calculations are usually performed along the lines  $\Delta$  and  $\Lambda$  – which connect the center  $\Gamma$  of the Brillouin zone with the centers  $X$  and  $L$  of the square and hexagonal shaped faces –, and perhaps for some other vectors along other characteristic directions. Figure 17.3 shows the band structure of aluminum calculated in this way.

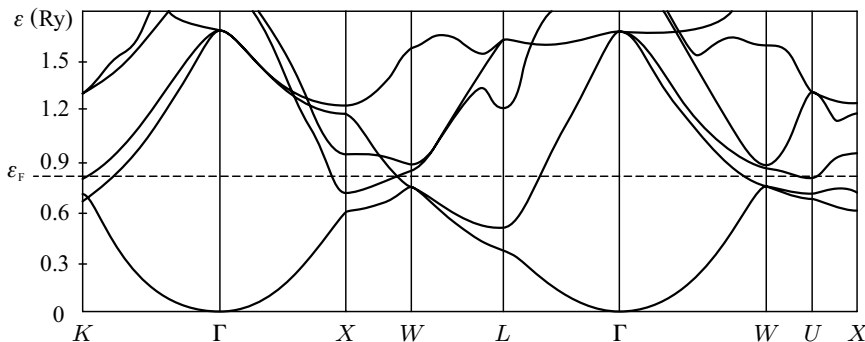


**Fig. 17.3.** Calculated band structure of aluminum along high-symmetry directions of the Brillouin zone

<sup>2</sup> G. DRESSELHAUS, 1955.



As the figure shows, if the band index were chosen in such a way that the energies are indexed in ascending order for any  $\mathbf{k}$  then break points would appear in the  $\varepsilon_{n\mathbf{k}}$  vs.  $\mathbf{k}$  plot (with  $n$  fixed) wherever two lines intersect. As has been mentioned before, we shall rather require that for a given band index the dispersion relation in  $\mathbf{k}$  lead to continuous, smooth curves. The dispersion curves of different bands may therefore intersect each other, and the energy regions covered by the bands may overlap.

However, bands can also overlap even when the dispersion curves – or in higher dimensions the  $\varepsilon_{n\mathbf{k}}$  (hyper)surfaces – do not intersect, nevertheless there are states whose energy is the same although they are associated with different points of the Brillouin zone and belong in different bands.

### 17.2.1 Reduced-, Repeated-, and Extended-Zone Schemes

As we have seen, the same energy eigenvalue is associated with equivalent  $\mathbf{k}$  vectors, it is therefore immaterial whether wave vectors defined in the Brillouin zone or in the primitive cell of the reciprocal lattice are used. With wave vectors reduced to the Brillouin zone, the energies of each band can be represented – occasionally separately – in the same Brillouin zone. This is the *reduced-zone scheme*.

Sometimes it is more practical not to restrict wave vectors to the Brillouin zone but use all equivalent vectors  $\mathbf{k} + \mathbf{G}$  as well. By virtue of (17.1.27) the band structure can then be represented by repeating all dispersion curves over the whole  $\mathbf{k}$ -space. This is the *repeated-zone scheme*.

Finally, the infinite number of solutions associated with a given  $\mathbf{k}$  can also be distributed among the infinite number of vectors  $\mathbf{k} + \mathbf{G}$  in such a way that one solution should belong to each equivalent vector. This can be achieved in two different ways. The first possibility is to draw the Brillouin zones around each lattice point, which gives an unambiguous filling of the entire space. Then, using a predefined – and, to a certain extent, arbitrary – procedure, a vector  $\mathbf{G}$  of the reciprocal lattice is assigned to each band index, and the states in that band are associated with the wave vectors in the Brillouin zone around that particular  $\mathbf{G}$ .

In the other, more commonly used method for distributing the band states among equivalent  $\mathbf{k}$  vectors, the notion of higher (second, third, etc.) Brillouin zones is introduced, and the reciprocal space is divided in another way. To this end, we shall generalize Dirichlet's procedure – mentioned in Section 5.1.4 in connection with the construction of the Wigner–Seitz cell, and which is also the method for constructing Brillouin zones in reciprocal space. In this generalization a selected lattice point of the reciprocal lattice is connected with all other lattice points of the reciprocal lattice, and the perpendicular bisecting planes of the segments are drawn. These planes are Bragg planes because any vector  $\mathbf{k}$  drawn from the selected reciprocal-lattice point to a point of the plane satisfies the Bragg condition (8.1.7). The division of the entire reciprocal space among higher Brillouin zones by means of the Bragg

planes is based on the criterion of how many Bragg planes need to be crossed (at least) to reach a particular region from the selected point.

The usual Brillouin zone around the selected point will be the first Brillouin zone. The second Brillouin zone will comprise those regions that can only be reached along a straight line from the selected point by intersecting one Bragg plane. In other words: the second zone comprises those regions that have a common boundary with the first zone.

The third Brillouin zone is made up of regions that have a common boundary with the second zone. To reach such regions from the selected starting point, two Bragg planes need to be crossed. In general: the  $n$ th Brillouin zone is reached by crossing  $n - 1$  Bragg planes. This division of the reciprocal space is shown in Fig. 17.4 for a two-dimensional square lattice.

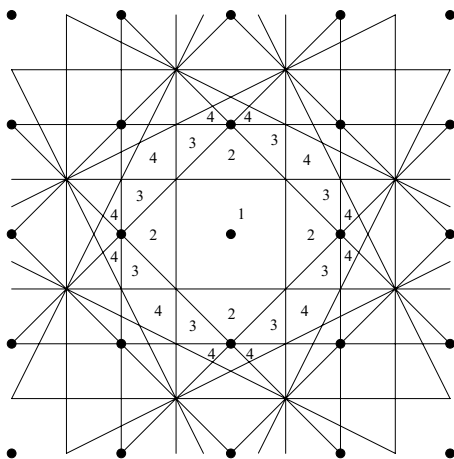


**Fig. 17.4.** Division of the reciprocal space of a square lattice to first, second, third, etc. Brillouin zones

Higher Brillouin zones may consist of disjoint parts. Nevertheless when these are translated through suitably chosen vectors of the reciprocal lattice, they are found to cover the first Brillouin zone precisely – that is, the total volume of each higher Brillouin zone is the same as that of the first. This is demonstrated in Fig. 17.5 where the parts of the second, third, and fourth Brillouin zones (marked by the corresponding numbers in the previous figure) are moved in such a way that they make up a square.

Figure 17.6 shows the external boundaries of the second, third, and fourth Brillouin zones of a simple cubic lattice, while Fig. 17.7 shows the external boundaries of the first and second Brillouin zones for face- and body-centered cubic lattices. Once again, each higher Brillouin zone has the same total volume as the first, and they can be reduced to the first Brillouin zone by suitable translations.

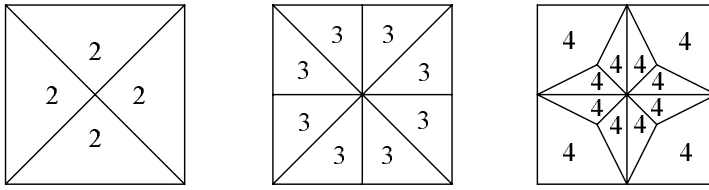


**Fig. 17.5.** Reduction of the second, third, and fourth Brillouin zones of a square lattice to the first zone

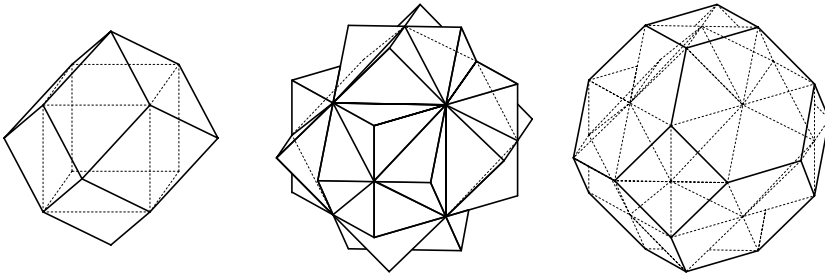


**Fig. 17.6.** External boundaries of the second, third, and fourth Brillouin zones for a simple cubic lattice

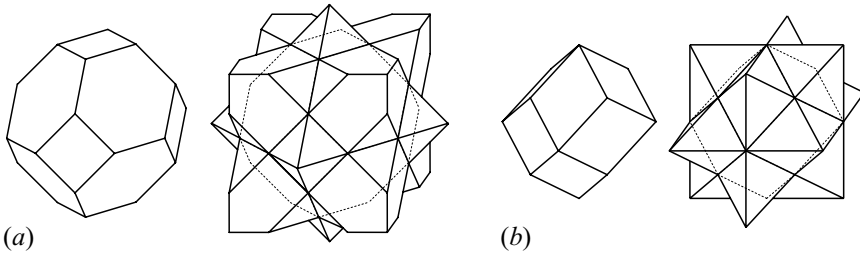


**Fig. 17.7.** External boundaries of the first and second Brillouin zones for (a) face-centered and (b) body-centered cubic lattices

The assignment of the states to the zones is then done simply by assigning the states of the first band to the wave vectors in the first Brillouin zone, the states of the second band to the wave vectors in the second Brillouin zone, and so forth. This is how the *extended-zone scheme* is obtained.

In Fig. 17.2 the band structure was plotted as a function of the reduced wave number in the Brillouin zone. The same band structure of the 40-atom chain represented in the repeated- and extended-zone schemes is shown in Fig. 17.8. For the latter the fourth band is outside the displayed region.

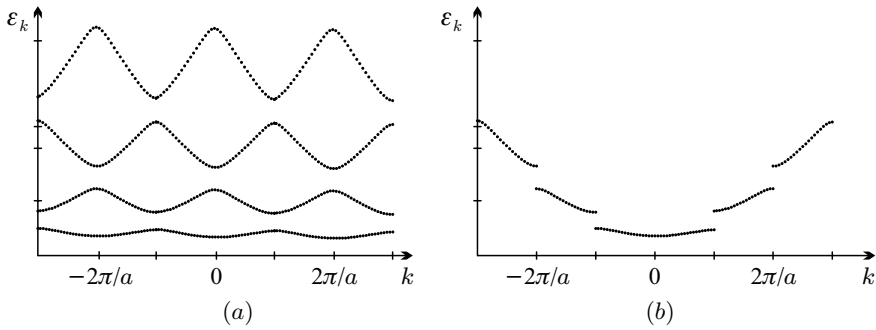


**Fig. 17.8.** The energy levels shown in Fig. 17.2 in the (a) repeated- and (b) extended-zone schemes

### 17.2.2 Constant-Energy Surfaces and the Fermi Surface

The energy of electron states can also be illustrated by specifying the regions of constant energy in  $\mathbf{k}$ -space. In two dimensions lines, while in three dimensions surfaces of constant energy are obtained. The constant-energy surfaces determined for a face-centered cubic lattice with a relatively weak potential are shown in Figure 17.9 for two different energies.

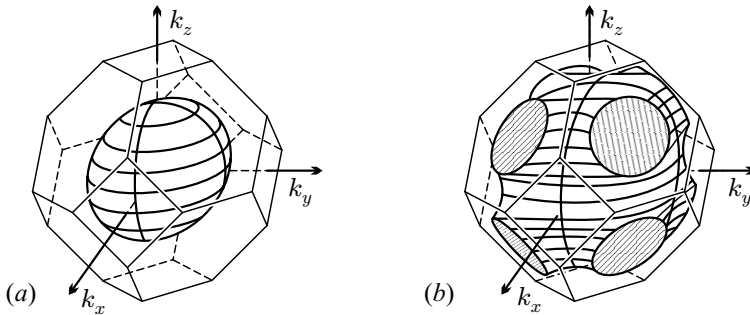


**Fig. 17.9.** Constant-energy surfaces in the band structure of a face-centered cubic crystal for two values of the energy

Among the constant-energy surfaces particularly important is the surface that contains those  $\mathbf{k}$  vectors for which the energy is the same as the zero-temperature value of the chemical potential. This energy is called the Fermi energy for Bloch states, too. Since in the ground state all the states whose energy is lower than the chemical potential are occupied while higher-energy states are empty, this surface separates occupied and unoccupied states in

$\mathbf{k}$ -space. This constant-energy surface is called the *Fermi surface*. As demonstrated for the Sommerfeld model, in the absence of a periodic potential this is just the surface of the Fermi sphere. However, the presence of a periodic potential can drastically distort the spherical shape of the Fermi surface – and, as we shall see, it can even disappear.

For a relatively small number of electrons only the states at the bottom of the lowest-lying band are occupied. The Fermi surface is then a simply connected continuous surface that deviates little from the spherical shape. When the number of electrons is increased, the surface may cease to be simply connected, as illustrated in Fig. 17.9(b). When the number of electrons exceeds twice the number of lattice points, electrons will certainly occupy the states of more than one band. In such cases more than one band can be partially filled. The Fermi surface separating occupied and unoccupied states must then be given for each of these – hence the Fermi surface is made up of several pieces. The reduced- and extended-zone schemes are both used to visualize them.

## 17.3 Metals, Insulators, Semiconductors

In the previous section it was assumed that there exist Bloch states whose energy is the same as the chemical potential. This is indeed the case when the Fermi energy (the chemical potential) lies inside a band (or several bands). Then the electrons that occupy states with slightly lower energies than the Fermi energy can be easily excited thermally or by an electric field into states with energies in excess of the Fermi energy. The behavior of such materials can be similar to what was presented for the free-electron model. Such materials are metals. As mentioned on page 75, their resistivity is typically on the order of  $10\text{ n}\Omega\text{ m}$  at room temperature, decreases with decreasing temperature, and in an ideal crystal it would even vanish at  $T = 0$ . A material is customarily considered metallic if its conductivity exceeds  $10^6\text{ (}\Omega\text{ m)}^{-1}$  (i.e., its resistivity  $\rho < 1\mu\Omega\text{ m}$ ).

However, the chemical potential may just as well be not inside a band but between two nonoverlapping bands, in which case there is no Bloch state whose energy is the same as the chemical potential. One cannot even speak of a Fermi surface then. This situation arises only when there are forbidden regions of finite width called *energy gaps* or *band gaps* such that the energies inside the gap do not appear as the energy of any band state. The most relevant band gap is the one that separates the bands that are filled completely in the ground state from those that are completely empty. By way of example, the band structure of diamond is shown in Fig. 17.10(a).

This can occur when the number of electrons per atom is even, and they completely fill one or more bands in the ground state, and the next, empty band is separated by a finite energy gap from the occupied ones. In such

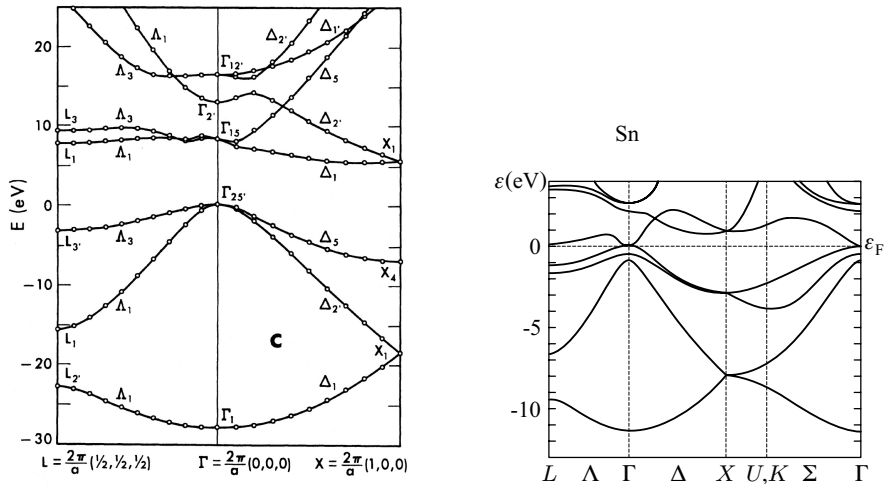


**Fig. 17.10.** Calculated band structures in high-symmetry directions of the Brillouin zone for (a) diamond [Reprinted with permission from W. Saslow, T. K. Bergstresser, and M. L. Cohen, *Phys. Rev. Lett.* **16**, 354 (1966). ©1966 by the American Physical Society] and (b) gray tin [Reprinted with permission from J. R. Chelikowsky and M. L. Cohen, *Phys. Rev. B* **14**, 556 (1976). ©1976 by the American Physical Society]

materials electric current starts to flow only above a certain (rather large) threshold voltage. They are called *insulators*. At  $T = 0$  the resistivity of insulators is infinitely large.

This implies that if the band structure is known, a sharp line can be drawn between metals and insulators: the chemical potential in the ground state is inside a band in the former and inside a gap in the latter. However, when physical properties measured at finite temperatures are considered, continuous variations are found. At finite temperatures those states whose energy is larger than the chemical potential can be partially filled by thermally excited electrons, and lower-energy states can be partially empty. Therefore, strictly speaking, the conductivity does not vanish even when the energy gap exceeds the thermal energy  $k_B T$ . A material is considered to be electrically insulating if its conductivity is less than  $10^{-8} (\Omega \text{ m})^{-1}$ . In general, those materials that are insulators at low temperatures remain insulators at room temperature, too. However, there is a class of materials whose conductivity vs. temperature plot has a jump at a certain temperature or changes several orders of magnitude in a narrow temperature range. This phenomenon is called the *metal-insulator transition*.

Among the materials whose band structure has a finite gap around the chemical potential particular behavior is observed in those for which the energy gap is larger than the thermal energy at room temperature but nonetheless sufficiently small, consequently electrons excited thermally across the gap

carry an electric current that can be easily measured and has substantial effects. Such materials are called *semiconductors*.

Compared to the usual values in metals, smaller conductivities are obtained when the energy gap is extremely narrow – or even nonexistent – around the Fermi energy but the electronic density of states is very low there. Materials featuring such a band structure are called *semimetals*. Examples include elements of the nitrogen group (group 15 [VA] of the periodic table): arsenic, antimony, and bismuth, as well as graphite, a modification of carbon (group 14 [IVA]). As listed in Table 16.2, the conductivity of bismuth is close to the lower limit set for metals. Gray tin is the example for vanishing gap at the Fermi energy, as shown in Fig. 17.10(b): the two bands touch each other at the Fermi energy. Nevertheless, on account of the low density of states, thermally excited electrons do not reach the states directly above the Fermi level but those in a somewhat higher-lying local minimum with a high density of states, therefore, from an electric point of view, gray tin is a semiconductor.

In materials that crystallize in a structure with a monatomic basis each band contains the same number of  $k$  states as there are lattice points. Among them those materials that have an odd number of electrons per atom behave electrically as metals since the topmost band that contains electrons in the ground state cannot be completely filled on account of spin degeneracy. Indeed, the alkali metals in the first column of the periodic table are all good metallic conductors. The single electron on the outermost  $s$ -shell in the atomic state finds itself in a band that is only half filled. The noble metals of group 11 (IB) and the elements of the boron group (group 13 [IIIA]) have more complex band structures, nonetheless they are metals – with the sole exception of boron. Boron itself crystallizes in a rhombohedral structure with a polyatomic basis, the chemical potential is inside a 1.5 eV wide gap, therefore it is a semiconductor.

Insulators and semiconductors are expected to be found among the elements of even-numbered columns of the periodic table, to the left and right of transition metals. However, elements of group 2 (IIA), alkaline-earth metals, are all metals, since the overlap of bands leads to the formation of two partially filled bands. At the other extremity of the periodic table nonmetallic elements are found. The halogens in group 17 (VIIA) and the noble gases in group 18 (VIIIA) are not even crystalline at room temperature.<sup>3</sup> Semiconductors should be looked for in groups 14 (IVA) and 16 (VIA).

Instead of their conductivity, materials can also be characterized by the number of charge carriers. In metals the room-temperature concentration of conduction electrons usually exceeds  $10^{22}/\text{cm}^3$ , while it is between  $10^{17}$  and  $10^{21}/\text{cm}^3$  in semimetals. It is even lower in semiconductors, e.g.,  $10^{13}/\text{cm}^3$  in germanium and  $10^{10}/\text{cm}^3$  in silicon at room temperature.

<sup>3</sup> In spite of their odd number of electrons, halogens are not metallic even at low temperatures as their centered monoclinic or orthorhombic lattices are decorated with polyatomic bases.

This classification of crystalline solids is based on the assumption that all interactions can be lumped into a periodic potential, and then the state of the electron system can be given as the superposition of one-particle states. However, this assumption is not always valid. Those insulators whose properties can be interpreted in this simple band picture are called band insulators or *Bloch–Wilson insulators*. Nevertheless under certain circumstances the interaction of electrons with lattice vibrations or with each other can also render the material insulator. We speak of *Peierls insulators* in the first case and *Mott insulators* in the second. Finally, disorder can also make the conductivity vanish. Such materials are called *Anderson insulators*. The study of their physical properties, which are essentially determined by the interactions, will be the subject of later chapters.

## 17.4 Bloch Electrons as Quasiparticles

Whether the thermodynamic properties are examined or the response to applied electromagnetic fields, real metals often show very similar qualitative behavior to a free electron gas. This is not surprising in view of the band structure constructed from one-particle states, however the question remains: how come electron–electron interactions can be lumped into a one-particle potential? This question will be revisited in Volume 3. Below we shall demonstrate that the system of electrons interacting with the periodic potential of the crystal can be described as a gas of fictitious noninteracting particles obeying the Fermi–Dirac statistics. These fermionic *quasiparticles* are called Bloch electrons. Quasiparticles are defined only inside solids, and their quantum mechanical state cannot be identified with any state of a single real electron, but they offer a simple physical interpretation of the behavior of the electron system. Using this picture we shall show that the thermodynamic properties of electrons moving in a periodic potential can be easily calculated using essentially a few parameters for simple metals.

### 17.4.1 Creation and Annihilation Operators of Bloch States

It is often more convenient to treat the electron system in the occupation-number formalism (second quantization). Following the prescriptions of Appendix H, we shall introduce the creation and annihilation operators of Bloch states,  $c_{n\mathbf{k}\sigma}^\dagger$  and  $c_{n\mathbf{k}\sigma}$ , where  $\sigma$  is the spin quantum number. These operators obey the fermionic anticommutation relations,

$$[c_{n\mathbf{k}\sigma}, c_{n'\mathbf{k}'\sigma'}^\dagger]_+ = \delta_{nn'}\delta_{\mathbf{k}\mathbf{k}'}\delta_{\sigma\sigma'} . \quad (17.4.1)$$

Using these operators the state of  $N_e$  electrons in which individual Bloch electrons occupy one-particle states associated with the wavefunctions  $\psi_{n_1\mathbf{k}_1\sigma_1}$ ,  $\psi_{n_2\mathbf{k}_2\sigma_2}, \dots$  (and which could also be written as a Slater determinant) can be expressed as



$$\Psi = c_{n_1 \mathbf{k}_1 \sigma_1}^\dagger c_{n_2 \mathbf{k}_2 \sigma_2}^\dagger \cdots c_{n_{N_e} \mathbf{k}_{N_e} \sigma_{N_e}}^\dagger |0\rangle, \quad (17.4.2)$$

where  $|0\rangle$  is the vacuum of Bloch electrons.

If the Hamiltonian of the system can be written as the sum of one-particle Hamiltonians over the individual particles – as was assumed in (17.1.2) – then, according to (H.2.9) and (H.2.10), it can be rewritten in the occupation-number representation as the following bilinear combination of creation and annihilation operators:

$$\mathcal{H} = \sum_{\substack{n n' \\ \mathbf{k} \mathbf{k}' \sigma \sigma'}} c_{n \mathbf{k} \sigma}^\dagger H(n, n', \mathbf{k}, \mathbf{k}', \sigma, \sigma') c_{n' \mathbf{k}' \sigma'}, \quad (17.4.3)$$

where  $H(n, n', \mathbf{k}, \mathbf{k}', \sigma, \sigma')$  is the matrix element of the one-particle Hamiltonian  $\mathcal{H}(\mathbf{r})$  between one-particle states:

$$H(n, n', \mathbf{k}, \mathbf{k}', \sigma, \sigma') = \int \psi_{n \mathbf{k} \sigma}^*(\mathbf{r}) \mathcal{H}(\mathbf{r}) \psi_{n' \mathbf{k}' \sigma'}(\mathbf{r}) d\mathbf{r}. \quad (17.4.4)$$

Since according to (17.1.3) the orthonormalized Bloch functions  $\psi_{n \mathbf{k} \sigma}(\mathbf{r})$  are the eigenfunctions of the one-particle Hamiltonian with energy eigenvalues  $\varepsilon_{n \mathbf{k}}$ ,

$$\boxed{\mathcal{H} = \sum_{n, \mathbf{k}, \sigma} \varepsilon_{n \mathbf{k}} c_{n \mathbf{k} \sigma}^\dagger c_{n \mathbf{k} \sigma}}. \quad (17.4.5)$$

The Hamiltonian of the electron system is that of a noninteracting gas of fermions (Bloch electrons) of energy  $\varepsilon_{n \mathbf{k}}$ . Compared to the gas of free electrons, the energy  $\hbar^2 k^2 / 2m_e$  containing the electron mass is replaced by  $\varepsilon_{n \mathbf{k}}$  obtained for Bloch electrons. In the ground state Bloch electrons fill the Fermi sea completely – that is, all states whose energy is smaller than the Fermi energy are occupied. At finite temperatures states above the Fermi energy may also be occupied. According to the Fermi–Dirac distribution function, the occupation probability – i.e., the mean number of electrons with wave vector  $\mathbf{k}$  and spin  $\sigma$  in the  $n$ th band – is given by

$$\langle n_{n \mathbf{k} \sigma} \rangle = \langle c_{n \mathbf{k} \sigma}^\dagger c_{n \mathbf{k} \sigma} \rangle = \frac{1}{e^{(\varepsilon_{n \mathbf{k}} - \mu) / k_B T} + 1}. \quad (17.4.6)$$

The variations of the momentum distribution function at finite temperature with respect to the ground-state distribution is interpreted as being due to the thermal excitation of fermionic quasiparticles.

### 17.4.2 Effective Mass of Bloch Electrons

At the bottom of the bands, close to the minimum, the dispersion relation of Bloch electrons can be approximated by a quadratic expression of the wave vectors. In a cubic crystal, when the minimum is at a high-symmetry point  $\mathbf{k}_0$ , the energy can be approximated by

$$\varepsilon_{\mathbf{k}} \approx \varepsilon_{\mathbf{k}_0} + A(\mathbf{k} - \mathbf{k}_0)^2. \quad (17.4.7)$$

By writing the coefficient  $A$  as

$$A = \frac{\hbar^2}{2m^*}, \quad (17.4.8)$$

the dispersion relation is similar to that of free electrons but the electron mass  $m_e$  is replaced by another value,  $m^*$ , which depends on the periodic potential and can also be defined as

$$\boxed{\frac{1}{m^*} = \frac{1}{\hbar^2} \frac{\partial^2 \varepsilon_{\mathbf{k}}}{\partial \mathbf{k}^2}}. \quad (17.4.9)$$

By analogy, this parameter is called the *effective mass* of the Bloch electron.

Naturally, the effective mass determined from (17.4.9) is different from the free electron mass, moreover, it takes different values in each band – and if there are several minima in the band, it also depends on the specific point of the Brillouin zone at which the second derivative is taken. The notion of effective mass is particularly useful when the electrons that determine the thermal properties of the crystal are in that region of a band where the quadratic approximation of the energy is justified. A barely filled metallic band or the conduction and valence bands in semiconductors are good examples. In these cases the system of Bloch electrons behaves just like a system of free electrons, except that the electron mass is replaced by an effective mass.

In noncubic crystals the dispersion relation is not spherically symmetric. If close to the minimum the local symmetry of the Brillouin zone is orthorhombic, the series expansion of the energy is

$$\varepsilon_{\mathbf{k}} \approx \varepsilon_{\mathbf{k}_0} + A_x(k_x - k_{0x})^2 + A_y(k_y - k_{0y})^2 + A_z(k_z - k_{0z})^2. \quad (17.4.10)$$

Rewriting this expression as

$$\varepsilon_{\mathbf{k}} \approx \varepsilon_{\mathbf{k}_0} + \frac{\hbar^2(k_x - k_{0x})^2}{2m_x^*} + \frac{\hbar^2(k_y - k_{0y})^2}{2m_y^*} + \frac{\hbar^2(k_z - k_{0z})^2}{2m_z^*}, \quad (17.4.11)$$

the behavior of the electrons is characterized by the triplet  $m_x^*$ ,  $m_y^*$ ,  $m_z^*$ . Even more generally, when it is sufficient to keep quadratic terms in the series expansion around the minimum, an inverse effective-mass tensor can be introduced instead of the scalar effective mass using the definition

$$\boxed{\left(\frac{1}{M^*}\right)_{\alpha\beta} = \frac{1}{\hbar^2} \frac{\partial^2 \varepsilon_{\mathbf{k}}}{\partial k_\alpha \partial k_\beta}}, \quad \alpha, \beta = x, y, z. \quad (17.4.12)$$

The energy of the band states then reads

$$\varepsilon_{\mathbf{k}} \approx \varepsilon_{\mathbf{k}_0} + \frac{\hbar^2}{2} \sum_{\alpha\beta} \left(\frac{1}{M^*}\right)_{\alpha\beta} (k_\alpha - k_{0\alpha})(k_\beta - k_{0\beta}). \quad (17.4.13)$$

The effective-mass tensor  $M^*$  is the inverse of the above-defined  $1/M^*$ . It takes a particularly simple form when the inverse mass tensor is diagonal: if

$$\frac{1}{M^*} = \begin{pmatrix} \frac{1}{m_1^*} & 0 & 0 \\ 0 & \frac{1}{m_2^*} & 0 \\ 0 & 0 & \frac{1}{m_3^*} \end{pmatrix} \quad (17.4.14)$$

then the effective-mass tensor is also diagonal and

$$M^* = \begin{pmatrix} m_1^* & 0 & 0 \\ 0 & m_2^* & 0 \\ 0 & 0 & m_3^* \end{pmatrix}. \quad (17.4.15)$$

### 17.4.3 Bloch Electrons and Holes

The description in terms of the effective mass is usually satisfactory at low band filling. We shall often encounter the opposite case where the band is almost completely filled and only a small number of states close to the top of the band remain unoccupied. This situation can be regarded as if some electrons in the vicinity of the maximum were removed from the completely filled band – that is, holes were generated.

When a band is completely filled with electrons the sum of the wave vectors  $\mathbf{k}$  of occupied states (i.e., the sum over the entire Brillouin zone) is zero:

$$\sum_{\mathbf{k} \in \text{BZ}} \mathbf{k} = 0. \quad (17.4.16)$$

Now let us remove an electron of wave vector  $\mathbf{k}_e$  from this completely filled band. The wave vector of this state,

$$\mathbf{k}_h = \sum_{\mathbf{k} \in \text{BZ}} \mathbf{k} - \mathbf{k}_e = -\mathbf{k}_e, \quad (17.4.17)$$

is just the negative of the electron's wave vector. When a hole is created, the change in the energy of the system is the negative of the energy of the removed particle, therefore the energy  $\varepsilon_h(\mathbf{k}_h)$  of the hole satisfies

$$\varepsilon_h(\mathbf{k}_h) = -\varepsilon(\mathbf{k}_e). \quad (17.4.18)$$

Provided that close to the top of the band the dispersion relation is isotropic, the leading correction of the expansion gives

$$\varepsilon_{\mathbf{k}} \approx \varepsilon_{\mathbf{k}_0} - A(\mathbf{k} - \mathbf{k}_0)^2, \quad A > 0. \quad (17.4.19)$$

According to the defining equation (17.4.9), the effective mass is negative for electrons with energies close to the maximum:

$$\frac{1}{m^*} = -\frac{2A}{\hbar^2}. \quad (17.4.20)$$

However, when hole energies are considered, the sign of the quadratic term is reversed, and the effective mass of the hole defined by

$$\frac{1}{m_h^*} = \frac{1}{\hbar^2} \frac{\partial^2 \varepsilon_h(\mathbf{k}_h)}{\partial \mathbf{k}_h^2} \quad (17.4.21)$$

is positive:

$$m_h^* = -m^*. \quad (17.4.22)$$

For general dispersion curves the inverse effective-mass tensor

$$\left( \frac{1}{M_h^*} \right)_{\alpha\beta} = -\frac{1}{\hbar^2} \frac{\partial^2 \varepsilon_{\mathbf{k}}}{\partial k_\alpha \partial k_\beta} \quad (17.4.23)$$

has to be used once again. If a band is almost completely filled, treating the small number of unoccupied electron states as positive-effective-mass holes proves to be convenient especially in the description of the dynamics of electrons and the discussion of semiconductors.

#### 17.4.4 Density of States for Bloch Electrons

Just like in the free-electron case, we shall often need the sum of some quantity  $g(\mathbf{k})$  – for example the energy – over occupied  $\mathbf{k}$ -space states in order to determine certain properties of the electron system. For large samples containing a great number of primitive cells the allowed values of  $\mathbf{k}$  fill the Brillouin zone densely, therefore the sum can be replaced by an integral. Considering the contribution of electrons in each band individually,

$$\boxed{\sum_{\mathbf{k}} g(\mathbf{k}) f_0(\varepsilon_{n\mathbf{k}}) \rightarrow \frac{V}{(2\pi)^3} \int g(\mathbf{k}) f_0(\varepsilon_{n\mathbf{k}}) d\mathbf{k}.} \quad (17.4.24)$$

In a lot of cases quantities that depend on the energy alone need to be summed, therefore we can once again introduce the density of states by stipulating that  $\rho_n(\varepsilon) d\varepsilon$  is the number of states in the  $n$ th band with energies between  $\varepsilon$  and  $\varepsilon + d\varepsilon$ . The  $\mathbf{k}$ -sum or  $\mathbf{k}$ -integral can then be rewritten as an energy integral of the density of states:

$$\sum_{\mathbf{k}\sigma} g(\varepsilon_{n\mathbf{k}}) f_0(\varepsilon_{n\mathbf{k}}) = V \int g(\varepsilon) f_0(\varepsilon) \rho_n(\varepsilon) d\varepsilon. \quad (17.4.25)$$

Following the steps in Chapter 12, where the phonon density of states was derived, we get

$$\rho_n(\varepsilon) = \frac{2}{(2\pi)^3} \int_{S(\varepsilon)} \frac{dS}{|\nabla_{\mathbf{k}} \varepsilon_{n\mathbf{k}}|}, \quad (17.4.26)$$

where the integral has to be evaluated for the constant-energy surface  $S(\varepsilon)$ . The factor two comes from the spin quantum number. The total electronic density of states is a sum over bands:

$$\rho(\varepsilon) = \sum_n \rho_n(\varepsilon). \quad (17.4.27)$$

If the energy of the electrons depends on spin, so does the density of states:

$$\rho_{n\sigma}(\varepsilon) = \frac{1}{(2\pi)^3} \int_{S(\varepsilon)} \frac{dS}{|\nabla_{\mathbf{k}} \varepsilon_{n\mathbf{k}\sigma}|}, \quad (17.4.28)$$

and the total density of states is then given by

$$\rho(\varepsilon) = \sum_{n\sigma} \rho_{n\sigma}(\varepsilon). \quad (17.4.29)$$

Just like for phonons, the Van Hove singularities discussed in Chapter 12 also appear in the electronic density of states. There is, nevertheless, an essential difference: for electrons the dispersion relation is quadratic at the bottom of the band, therefore a square-root singularity ( $P_0$ -type critical point) appears at the bottom of each band. It is quite natural that each band has a minimum and a maximum, i.e., the density of states features a  $P_0$ - and a  $P_3$ -type point. It can also be shown that each band has at least three  $P_1$ - and three  $P_2$ -type critical points as well. As we shall see in the tight-binding approximation, the simple cubic crystal provides an example for the minimum number of critical points if the dispersion relation is approximated by

$$\varepsilon_{\mathbf{k}} = \alpha [3 - \cos k_x a - \cos k_y a - \cos k_z a]. \quad (17.4.30)$$

The minimum is at the center  $\Gamma$  of the Brillouin zone, and the maximum is at the corner points  $R$ .  $P_1$ -type saddle points are found at the face centers  $X$ , since within the face the dispersion relation has its minimum at the center, while in the perpendicular direction it has its maximum there. On the other hand,  $P_2$ -type saddle points are found at the edge centers, since the dispersion relation along the edge has its minimum there, while it has its maximum in the same point along the lines joining the centers of the two adjacent faces.

If in the general case the dispersion relation transformed to the principal axes can be approximated by

$$\varepsilon_{\mathbf{k}} = \varepsilon_{\min} + \frac{\hbar^2 k_1^2}{2m_1^*} + \frac{\hbar^2 k_2^2}{2m_2^*} + \frac{\hbar^2 k_3^2}{2m_3^*} \quad (17.4.31)$$

in the vicinity of the minimum, then the density of states is

$$\rho(\varepsilon) = \frac{\sqrt{2}}{\pi^2 \hbar^3} (m_1^* m_2^* m_3^*)^{1/2} \sqrt{\varepsilon - \varepsilon_{\min}}. \quad (17.4.32)$$

If the dispersion relation can be written as

$$\varepsilon_{\mathbf{k}} = \varepsilon_{\max} - \frac{\hbar^2 k_1^2}{2m_1^*} - \frac{\hbar^2 k_2^2}{2m_2^*} - \frac{\hbar^2 k_3^2}{2m_3^*} \quad (17.4.33)$$

in the vicinity of the maximum, then, by the same token, the density of states reads

$$\rho(\varepsilon) = \frac{\sqrt{2}}{\pi^2 \hbar^3} (m_1^* m_2^* m_3^*)^{1/2} \sqrt{\varepsilon_{\max} - \varepsilon}. \quad (17.4.34)$$

Around a  $P_1$ -type saddle point, where the dispersion relation is

$$\varepsilon_{\mathbf{k}} = \varepsilon_c + \frac{\hbar^2 k_1^2}{2m_1^*} + \frac{\hbar^2 k_2^2}{2m_2^*} - \frac{\hbar^2 k_3^2}{2m_3^*}, \quad (17.4.35)$$

the density of states has a square-root-type energy dependence in the region  $\varepsilon < \varepsilon_c$ :

$$\rho(\varepsilon) = C - \frac{\sqrt{2}}{\pi^2 \hbar^3} (m_1^* m_2^* m_3^*)^{1/2} \sqrt{\varepsilon_c - \varepsilon}. \quad (17.4.36)$$

For  $P_2$ -type saddle points a similar formula is obtained for energies above  $\varepsilon_c$ :

$$\rho(\varepsilon) = C - \frac{\sqrt{2}}{\pi^2 \hbar^3} (m_1^* m_2^* m_3^*)^{1/2} \sqrt{\varepsilon - \varepsilon_c}. \quad (17.4.37)$$

These formulas are straightforward to derive from the expressions for the Van Hove singularities for phonons established in Chapter 12: one has to substitute  $\alpha_1 = \hbar^2/2m_1^*$ ,  $\alpha_2 = \hbar^2/2m_2^*$ ,  $\alpha_3 = \hbar^2/2m_3^*$ , and include an extra factor of two arising from the electron spin.

Just like for phonons, the density of states features an inverse-square-root singularity at the bottom and top of the band in one-dimensional electron systems. In two-dimensional systems a logarithmic singularity appears at the energy associated with the saddle point:

$$\rho(\varepsilon) = C - \frac{1}{\pi^2 \hbar^2} (m_1^* m_2^*)^{1/2} \ln \left| 1 - \frac{\varepsilon}{\varepsilon_c} \right| + \mathcal{O}(\varepsilon - \varepsilon_c), \quad (17.4.38)$$

but at the energy of the bottom of the band the density of states jumps from zero to a finite value, and at the energy of the top of the band it drops from a finite value to zero.

### 17.4.5 Specific Heat and Susceptibility of Bloch Electrons

Bloch electrons also obey the Fermi–Dirac statistics at finite temperatures. By repeating the steps of the procedure for free electrons, the thermal energy and specific heat of electrons moving in a periodic potential can be determined.

Once again, we start with (16.2.88), however  $\varepsilon_{\mathbf{k}}$  is the energy of Bloch electrons and  $\rho(\varepsilon)$  the density of states of Bloch electrons this time. If the variation of the density of states is so slow in a region of width  $k_{\text{B}}T$  around the Fermi energy that it is justified to keep only the leading order term in the Sommerfeld expansion, then the specific heat takes the same form as (16.2.91):

$$c_{\text{el}} = \frac{\pi^2}{3} k_{\text{B}}^2 T \rho(\varepsilon_{\text{F}}), \quad (17.4.39)$$

where  $\rho(\varepsilon_{\text{F}})$  is the Bloch electron density of states at the Fermi energy. This can be understood relatively simply. Because of the Fermi–Dirac statistics, the thermal properties are determined by electrons whose energies are within a few times  $k_{\text{B}}T$  of the Fermi energy. As  $k_{\text{B}}T \ll \varepsilon_{\text{F}}$  at the usual temperatures, the specific heat is independent of the density of states far from the Fermi energy.

When the dispersion relation of Bloch electrons can be approximated by a quadratic function and the effective mass is a scalar, the coefficient of the linear term in the specific heat can be expressed by the effective mass just like in (16.2.92):

$$\gamma = \frac{k_{\text{B}}^2 m^*}{3\hbar^2} (3\pi^2 n_{\text{e}})^{1/3}. \quad (17.4.40)$$

In noncubic systems, where the dispersion relation must be given in terms of an effective-mass tensor rather than a single scalar parameter, the density of states has to be determined using (17.4.26) as an integral over the Fermi surface. It can be shown that the density of states can be recast in the same form as for free electrons but the electron mass is replaced by

$$m_{\text{ds}}^* = [\det(m_{ij}^*)]^{1/3}, \quad (17.4.41)$$

which corresponds to the combination

$$m_{\text{ds}}^* = (m_x^* m_y^* m_z^*)^{1/3} \quad (17.4.42)$$

in the orthorhombic case. This quantity is called the *density-of-states mass* in order to distinguish it from other combinations encountered in other physical quantities. Since this effective mass appears in the specific heat, the term *thermal mass* is also used.

This explains in part why the Sommerfeld coefficient (the proportionality factor of the temperature in the specific heat) of metals differs from the free-electron value. Nevertheless, the quantitative understanding of the so-called heavy-fermionic behavior, the extremely large effective mass, requires a more precise account of electron–electron interactions.

To determine the Pauli susceptibility arising from the spins of Bloch electrons, the calculation performed in the free-electron model is repeated. If the density of states varies little over a region of width  $\mu_{\text{B}}B$  around the Fermi energy, a similar formula is found:

$$\chi_P = \frac{1}{4}\mu_0(g_e\mu_B)^2\rho(\varepsilon_F), \quad (17.4.43)$$

with the single difference that the density of states at the Fermi energy is now that of the Bloch electrons. Therefore the periodic potential modifies the Pauli susceptibility, too, through the effective mass of Bloch electrons. As the same effective mass appears in the specific heat and the susceptibility, the Wilson ratio for noninteracting Bloch electrons is the same as for free electrons.

## 17.5 Wannier States

The one-particle wavefunction of electrons was written in the Bloch form in the previous sections. However, this is not the only possibility: in certain cases another representation is more practical.

### 17.5.1 Wannier Functions

We shall make use of the previously established relationship

$$\psi_{n,\mathbf{k}+\mathbf{G}}(\mathbf{r}) = e^{i(\mathbf{k}+\mathbf{G})\cdot\mathbf{r}} u_{n,\mathbf{k}+\mathbf{G}}(\mathbf{r}) = e^{i\mathbf{k}\cdot\mathbf{r}} u_{n\mathbf{k}}(\mathbf{r}) = \psi_{n\mathbf{k}}(\mathbf{r}), \quad (17.5.1)$$

which states that when  $\psi_{n\mathbf{k}}(\mathbf{r})$  is considered as a function of  $\mathbf{k}$  at a fixed  $\mathbf{r}$ , it is periodic in the reciprocal lattice. It can therefore be expanded into a Fourier series; the vectors that appear in this representation are the translation vectors of the reciprocal of the reciprocal lattice – that is, the lattice vectors of the original direct lattice. A convenient choice of normalization is

$$\psi_{n\mathbf{k}}(\mathbf{r}) = \frac{1}{\sqrt{N}} \sum_{\mathbf{R}_j} \phi_n(\mathbf{r}, \mathbf{R}_j) e^{i\mathbf{k}\cdot\mathbf{R}_j}. \quad (17.5.2)$$

Making use of (C.1.47) leads to

$$\phi_n(\mathbf{r}, \mathbf{R}_j) = \frac{1}{\sqrt{N}} \sum_{\mathbf{k} \in \text{BZ}} e^{-i\mathbf{k}\cdot\mathbf{R}_j} \psi_{n\mathbf{k}}(\mathbf{r}) \quad (17.5.3)$$

for the Fourier coefficients. In what follows, even when it is not explicitly indicated, summation over  $\mathbf{k}$  refers to summation over the wave vectors in the Brillouin zone.

We shall first demonstrate that the above-defined  $\phi_n(\mathbf{r}, \mathbf{R}_j)$  is indeed a function of  $\mathbf{r} - \mathbf{R}_j$  alone. To this end we shall translate both  $\mathbf{R}_j$  and  $\mathbf{r}$  by  $\mathbf{t}_m$ , and make use of the translational properties of  $\psi_{n\mathbf{k}}(\mathbf{r})$ :



$$\begin{aligned}
\phi_n(\mathbf{r} + \mathbf{t}_m, \mathbf{R}_j + \mathbf{t}_m) &= \frac{1}{\sqrt{N}} \sum_{\mathbf{k}} e^{-i\mathbf{k} \cdot (\mathbf{R}_j + \mathbf{t}_m)} \psi_{n\mathbf{k}}(\mathbf{r} + \mathbf{t}_m) \\
&= \frac{1}{\sqrt{N}} \sum_{\mathbf{k}} e^{-i\mathbf{k} \cdot (\mathbf{R}_j + \mathbf{t}_m)} e^{i\mathbf{k} \cdot \mathbf{t}_m} \psi_{n\mathbf{k}}(\mathbf{r}) \\
&= \frac{1}{\sqrt{N}} \sum_{\mathbf{k}} e^{-i\mathbf{k} \cdot \mathbf{R}_j} \psi_{n\mathbf{k}}(\mathbf{r}) \\
&= \phi_n(\mathbf{r}, \mathbf{R}_j).
\end{aligned} \tag{17.5.4}$$

By choosing  $\mathbf{t}_m = -\mathbf{R}_j$ ,

$$\phi_n(\mathbf{r}, \mathbf{R}_j) = \phi_n(\mathbf{r} - \mathbf{R}_j, 0), \tag{17.5.5}$$

which shows that the genuine variable is the difference of  $\mathbf{r}$  and  $\mathbf{R}_j$ . The functions  $\phi_n(\mathbf{r} - \mathbf{R}_j)$  are called *Wannier functions*.<sup>4</sup> According to (17.5.3), they can be related to the Bloch function by

$$\begin{aligned}
\phi_n(\mathbf{r} - \mathbf{R}_j) &= \frac{1}{\sqrt{N}} \sum_{\mathbf{k}} e^{-i\mathbf{k} \cdot \mathbf{R}_j} \psi_{n\mathbf{k}}(\mathbf{r}) \\
&= \frac{1}{\sqrt{N}} \sum_{\mathbf{k}} e^{i\mathbf{k} \cdot (\mathbf{r} - \mathbf{R}_j)} u_{n\mathbf{k}}(\mathbf{r}),
\end{aligned} \tag{17.5.6}$$

while the inverse relationship is

$$\psi_{n\mathbf{k}}(\mathbf{r}) = \frac{1}{\sqrt{N}} \sum_{\mathbf{R}_j} e^{i\mathbf{k} \cdot \mathbf{R}_j} \phi_n(\mathbf{r} - \mathbf{R}_j), \tag{17.5.7-a}$$

$$u_{n\mathbf{k}}(\mathbf{r}) = \frac{1}{\sqrt{N}} \sum_{\mathbf{R}_j} e^{-i\mathbf{k} \cdot (\mathbf{r} - \mathbf{R}_j)} \phi_n(\mathbf{r} - \mathbf{R}_j). \tag{17.5.7-b}$$

It is readily seen that the functions  $\psi_{n\mathbf{k}}(\mathbf{r})$  expressed in terms of the Wannier functions satisfy the conditions (6.2.5) and (17.1.6) imposed on the Bloch functions. Taking the function at the position translated through  $\mathbf{t}_m$ ,

$$\psi_{n\mathbf{k}}(\mathbf{r} + \mathbf{t}_m) = \frac{1}{\sqrt{N}} \sum_{\mathbf{R}_j} \phi_n(\mathbf{r} + \mathbf{t}_m - \mathbf{R}_j) e^{i\mathbf{k} \cdot \mathbf{R}_j}. \tag{17.5.8}$$

Indexing the sum by the translated lattice point  $\mathbf{R}_l = \mathbf{R}_j - \mathbf{t}_m$  instead of the original  $\mathbf{R}_j$ , the sum remains unaltered on account of the periodic boundary conditions, thus

$$\psi_{n\mathbf{k}}(\mathbf{r} + \mathbf{t}_m) = \frac{1}{\sqrt{N}} \sum_{\mathbf{R}_l} \phi_n(\mathbf{r} - \mathbf{R}_l) e^{i\mathbf{k} \cdot (\mathbf{R}_l + \mathbf{t}_m)} = e^{i\mathbf{k} \cdot \mathbf{t}_m} \psi_{n\mathbf{k}}(\mathbf{r}). \tag{17.5.9}$$

---

<sup>4</sup> G. H. WANNIER, 1937.

Whether the Bloch functions or the Wannier representation is used, we have a complete orthogonal set of wavefunctions, since the orthogonality of the Bloch functions implies the orthogonality of the Wannier functions associated with different bands and lattice points:

$$\begin{aligned} \int \phi_n^*(\mathbf{r} - \mathbf{R}_j) \phi_{n'}(\mathbf{r} - \mathbf{R}_{j'}) d\mathbf{r} &= \frac{1}{N} \sum_{\mathbf{k}, \mathbf{k}'} \int e^{i(\mathbf{k} \cdot \mathbf{R}_j - \mathbf{k}' \cdot \mathbf{R}_{j'})} \psi_{n\mathbf{k}}^*(\mathbf{r}) \psi_{n'\mathbf{k}'}(\mathbf{r}) d\mathbf{r} \\ &= \frac{1}{N} \sum_{\mathbf{k}} e^{i\mathbf{k} \cdot (\mathbf{R}_j - \mathbf{R}_{j'})} \delta_{n, n'} \\ &= \delta_{\mathbf{R}_j, \mathbf{R}_{j'}} \delta_{n, n'}. \end{aligned} \quad (17.5.10)$$

The completeness of the Wannier functions can be demonstrated along the same lines:

$$\sum_{n, \mathbf{R}_j} \phi_n^*(\mathbf{r} - \mathbf{R}_j) \phi_n(\mathbf{r}' - \mathbf{R}_j) = \delta(\mathbf{r} - \mathbf{r}'). \quad (17.5.11)$$

Since the phase of Wannier functions can be chosen arbitrarily, it is possible to construct Wannier functions  $\phi_n(\mathbf{r} - \mathbf{R}_j)$  that take large values only around the lattice point  $\mathbf{R}_j$ , and drop off exponentially with distance in other cells. To demonstrate this, consider a simple example. For free electrons the function  $u_{n\mathbf{k}}(\mathbf{r})$  appearing in the Bloch function is independent of  $\mathbf{k}$ :  $e^{i\mathbf{G}_n \cdot \mathbf{r}}$ . Assuming a slightly more general but still  $\mathbf{k}$ -independent function  $u_n(\mathbf{r})$ , the Wannier functions that correspond to the Bloch functions

$$\psi_{n\mathbf{k}}(\mathbf{r}) = \frac{1}{\sqrt{V}} e^{i\mathbf{k} \cdot \mathbf{r}} u_n(\mathbf{r}) \quad (17.5.12)$$

can be determined exactly:

$$\begin{aligned} \phi_n(\mathbf{r} - \mathbf{R}_j) &= \frac{1}{\sqrt{NV}} \sum_{\mathbf{k}} e^{-i\mathbf{k} \cdot \mathbf{R}_j} e^{i\mathbf{k} \cdot \mathbf{r}} u_n(\mathbf{r}) \\ &= \frac{1}{N\sqrt{v}} \sum_{\mathbf{k}} e^{i\mathbf{k} \cdot (\mathbf{r} - \mathbf{R}_j)} u_n(\mathbf{r}) = \Phi(\mathbf{r} - \mathbf{R}_j) u_n(\mathbf{r}), \end{aligned} \quad (17.5.13)$$

where  $\Phi$  depends on the lattice constants  $a, b, c$  as

$$\Phi(\mathbf{r}) = \frac{1}{\sqrt{v}} \frac{\sin \pi x/a}{\pi x/a} \frac{\sin \pi y/b}{\pi y/b} \frac{\sin \pi z/c}{\pi z/c}. \quad (17.5.14)$$

It is readily seen that the Wannier function drops off with increasing distance, while oscillating sinusoidally with a period of twice the lattice constant. The Wannier functions are usually well localized in space for more realistic functions  $u_{n\mathbf{k}}(\mathbf{r})$  as well.

The Wannier states are not eigenstates of the one-particle Hamiltonian;  $\mathcal{H}$  couples Wannier functions associated with different lattice points but with the same band. Using (17.1.3),

$$\begin{aligned}
\mathcal{H} \phi_n(\mathbf{r} - \mathbf{R}_j) &= \mathcal{H} \frac{1}{\sqrt{N}} \sum_{\mathbf{k}} e^{-i\mathbf{k} \cdot \mathbf{R}_j} \psi_{n\mathbf{k}}(\mathbf{r}) \\
&= \frac{1}{\sqrt{N}} \sum_{\mathbf{k}} e^{-i\mathbf{k} \cdot \mathbf{R}_j} \varepsilon_{n\mathbf{k}} \psi_{n\mathbf{k}}(\mathbf{r}) \\
&= \frac{1}{N} \sum_{\mathbf{k}} e^{-i\mathbf{k} \cdot \mathbf{R}_j} \varepsilon_{n\mathbf{k}} \sum_{\mathbf{R}_l} e^{i\mathbf{k} \cdot \mathbf{R}_l} \phi_n(\mathbf{r} - \mathbf{R}_l).
\end{aligned} \tag{17.5.15}$$

This can be rewritten as

$$\mathcal{H} \phi_n(\mathbf{r} - \mathbf{R}_j) = \sum_{\mathbf{R}_l} t_{n,jl} \phi_n(\mathbf{r} - \mathbf{R}_l) \tag{17.5.16}$$

with

$$t_{n,jl} = \frac{1}{N} \sum_{\mathbf{k}} \varepsilon_{n\mathbf{k}} e^{i\mathbf{k} \cdot (\mathbf{R}_l - \mathbf{R}_j)}. \tag{17.5.17}$$

The orthonormality of the Wannier functions implies

$$t_{n,jl} = \int \phi_n^*(\mathbf{r} - \mathbf{R}_l) \mathcal{H}(\mathbf{r}) \phi_n(\mathbf{r} - \mathbf{R}_j) d\mathbf{r}. \tag{17.5.18}$$

Since the one-particle Hamiltonian is local, this coefficient vanishes unless the Wannier functions of the two lattice points overlap. Consequently it is often sufficient to consider only nearest neighbors and choose the Wannier function  $\phi_n(\mathbf{r} - \mathbf{R}_j)$  as the wavefunction of a core electron of the atom at  $\mathbf{R}_j$ , even though the orthogonality is lost with this choice.

### 17.5.2 Creation and Annihilation Operators of Wannier States

The creation and annihilation operators ( $c_{nj\sigma}^\dagger$  and  $c_{nj\sigma}$ ) can be introduced for Wannier states as well; in this case they change the occupation of the Wannier state at  $\mathbf{R}_j$  in the  $n$ th band by adding or removing an electron. In terms of these operators the Hamiltonian reads

$$\mathcal{H} = \sum_{n,\sigma} \sum_{j,l} t_{n,jl} c_{nl\sigma}^\dagger c_{nj\sigma}. \tag{17.5.19}$$

In this representation the Hamiltonian is nondiagonal. It describes the hopping of an electron in the Wannier state centered on the  $j$ th atom to a state centered on the  $l$ th atom. The probability of transition is the absolute square of the *hopping matrix element*  $t_{n,jl}$ .

Using the creation and annihilation operators of Bloch electrons means working in reciprocal space, while using those of the Wannier states means working in real space. The two representations are related by the discrete Fourier transforms

$$c_{nj\sigma}^\dagger = \frac{1}{\sqrt{N}} \sum_{\mathbf{k}} c_{n\mathbf{k}\sigma}^\dagger e^{-i\mathbf{k}\cdot\mathbf{R}_j}, \quad c_{nj\sigma} = \frac{1}{\sqrt{N}} \sum_{\mathbf{k}} c_{n\mathbf{k}\sigma} e^{i\mathbf{k}\cdot\mathbf{R}_j} \quad (17.5.20)$$

and

$$c_{n\mathbf{k}\sigma}^\dagger = \frac{1}{\sqrt{N}} \sum_{\mathbf{R}_j} c_{nj\sigma}^\dagger e^{i\mathbf{k}\cdot\mathbf{R}_j}, \quad c_{n\mathbf{k}\sigma} = \frac{1}{\sqrt{N}} \sum_{\mathbf{R}_j} c_{nj\sigma} e^{-i\mathbf{k}\cdot\mathbf{R}_j}, \quad (17.5.21)$$

in analogy with the mutual relations between Bloch and Wannier functions. These expressions can also be viewed as unitary transformations that diagonalize the Hamiltonian (17.5.19). This transformation also establishes the relationship between the energy of Bloch electrons and the hopping matrix elements (17.5.17):

$$\varepsilon_{n\mathbf{k}} = \sum_{\mathbf{R}_l} t_{n,jl} e^{-i\mathbf{k}\cdot(\mathbf{R}_l - \mathbf{R}_j)}. \quad (17.5.22)$$

## 17.6 Electron States Around Impurities

Before turning to the subject matter of the next chapters, the technical details of computing the band structure in an ideal crystal, it should be noted that only in ideal crystals do the Bloch and Wannier states exist in the form presented in the foregoing. In real materials impurities and defects are always present, and the electronic spectrum is therefore modified with respect to the ideal case. Adapting the procedure used in the study of localized lattice vibrations, it can be demonstrated that the energies of the  $N$  electron states making up the quasicontinuous band are modified in such a way that  $N - 1$  states remain inside the original band but one state can move outside. The difference with localized lattice vibrations is that the bound state can appear below or above the band (depending on whether the potential is attractive or repulsive). The spectrum of free electrons showed a similar pattern in the vicinity of an impurity, however, the free-electron spectrum being unbounded from above, bound states appeared only for attractive potentials, at negative energies. Below, we shall generalize the free-electron results to electrons moving in a periodic potential.

Suppose that an impurity atom at lattice site  $\mathbf{R}_0$  gives rise to an additional short-range potential  $V(\mathbf{r} - \mathbf{R}_0)$  relative to the periodic potential  $U(\mathbf{r})$  of the ideal crystal. Since the impurity breaks discrete translational symmetry, the states can no longer be characterized by a wave vector  $\mathbf{k}$ . Using an index  $\mu$  as quantum number, the Schrödinger equation that determines the electron states reads

$$\left[ -\frac{\hbar^2}{2m_e} \nabla^2 + U(\mathbf{r}) + V(\mathbf{r} - \mathbf{R}_0) \right] \psi_\mu(\mathbf{r}) = \varepsilon_\mu \psi_\mu(\mathbf{r}). \quad (17.6.1)$$

Suppose, furthermore, that the electron states of the ideal crystal – that is, the eigenfunctions and eigenvalues of the Schrödinger equation

$$\mathcal{H}_0\psi_{n\mathbf{k}}(\mathbf{r}) \equiv \left[ -\frac{\hbar^2}{2m_e}\nabla^2 + U(\mathbf{r}) \right] \psi_{n\mathbf{k}}(\mathbf{r}) = \varepsilon_{n\mathbf{k}}\psi_{n\mathbf{k}}(\mathbf{r}) \quad (17.6.2)$$

are known.

Equation (17.6.1) can be solved much in the same manner as (16.4.2), which describes the interaction of a free electron with an impurity. We find

$$\psi_\mu(\mathbf{r}) = \psi_{n\mathbf{k}}(\mathbf{r}) + \int G_{\varepsilon_\mu}(\mathbf{r}, \mathbf{r}') V(\mathbf{r}') \psi_\mu(\mathbf{r}') d\mathbf{r}', \quad (17.6.3)$$

where now the Green function  $G_\varepsilon(\mathbf{r}, \mathbf{r}')$  is the solution of

$$(\varepsilon - \mathcal{H}_0)G_\varepsilon(\mathbf{r}, \mathbf{r}') \equiv \left[ \varepsilon + \frac{\hbar^2}{2m_e}\nabla^2 - U(\mathbf{r}) \right] G_\varepsilon(\mathbf{r}, \mathbf{r}') = \delta(\mathbf{r} - \mathbf{r}'). \quad (17.6.4)$$

Expanding the Green function in terms of Bloch states as

$$G_\varepsilon(\mathbf{r} - \mathbf{r}') = \sum_{n\mathbf{k}} a_{n\mathbf{k}}(\mathbf{r}') \psi_{n\mathbf{k}}(\mathbf{r}), \quad (17.6.5)$$

and substituting this form into the equation for the Green function, the eigenvalue equation

$$\left[ -\frac{\hbar^2}{2m_e}\nabla^2 + U(\mathbf{r}) - \varepsilon_{n\mathbf{k}} \right] \psi_{n\mathbf{k}}(\mathbf{r}) = 0 \quad (17.6.6)$$

of the Bloch states and the orthogonality of Bloch functions imply that

$$a_{n\mathbf{k}}(\mathbf{r}') = \frac{\psi_{n\mathbf{k}}^*(\mathbf{r}')}{\varepsilon - \varepsilon_{n\mathbf{k}}}, \quad (17.6.7)$$

or

$$G_\varepsilon(\mathbf{r} - \mathbf{r}') = \sum_{n\mathbf{k}} \frac{\psi_{n\mathbf{k}}^*(\mathbf{r}') \psi_{n\mathbf{k}}(\mathbf{r})}{\varepsilon - \varepsilon_{n\mathbf{k}}}. \quad (17.6.8)$$

The wavefunction can then be written as

$$\psi_\mu(\mathbf{r}) = \psi_{n\mathbf{k}}(\mathbf{r}) + \sum_{n'\mathbf{k}'} \int \frac{\psi_{n'\mathbf{k}'}(\mathbf{r}) \psi_{n'\mathbf{k}'}^*(\mathbf{r}')}{\varepsilon - \varepsilon_{n'\mathbf{k}'} + i\alpha} V(\mathbf{r}') \psi_\mu(\mathbf{r}') d\mathbf{r}', \quad (17.6.9)$$

where  $\alpha$  is an infinitesimally small positive quantity that ensures the required analytic properties.

If the influence of the potential is limited to the vicinity of the impurity, as has been assumed, then it is more convenient to use Wannier functions than Bloch functions to calculate the matrix element. If the impurity is located at  $\mathbf{R}_0$  then only the Wannier functions associated with the same lattice point have nonvanishing matrix elements, and among them the matrix element of the transition into the same band is the most important. Keeping only this one, we have

$$\int \phi_n^*(\mathbf{r} - \mathbf{R}_j) V(\mathbf{r} - \mathbf{R}_0) \phi_{n'}(\mathbf{r} - \mathbf{R}_{j'}) d\mathbf{r} = V_{nn} \delta_{nn'} \delta(\mathbf{R}_j - \mathbf{R}_0) \delta(\mathbf{R}_{j'} - \mathbf{R}_0), \quad (17.6.10)$$

which is tantamount to stipulating that scattering by the impurity does not couple states in different bands. The state  $\psi_\mu$  can then be expanded in Wannier states associated with a single band:

$$\psi_\mu(\mathbf{r}) = \frac{1}{\sqrt{N}} \sum_j c(\mathbf{R}_j) \phi_n(\mathbf{r} - \mathbf{R}_j). \quad (17.6.11)$$

Substituting this into (17.6.9), and using an expansion in Wannier functions rather than Bloch functions,

$$c(\mathbf{R}_j) = e^{i\mathbf{k} \cdot \mathbf{R}_j} + \frac{1}{N} \sum_{\mathbf{k}'} \frac{e^{i\mathbf{k}' \cdot (\mathbf{R}_j - \mathbf{R}_0)}}{\varepsilon - \varepsilon_{n\mathbf{k}'} + i\alpha} V_{nn} c(\mathbf{R}_0). \quad (17.6.12)$$

The solution for  $\mathbf{R}_j = \mathbf{R}_0$  is

$$c(\mathbf{R}_0) = \frac{e^{i\mathbf{k} \cdot \mathbf{R}_0}}{1 - V_{nn} \frac{1}{N} \sum_{\mathbf{k}'} \frac{1}{\varepsilon - \varepsilon_{n\mathbf{k}'} + i\alpha}}. \quad (17.6.13)$$

The sum over  $\mathbf{k}'$  can be replaced by the energy integral

$$\begin{aligned} \frac{1}{N} \sum_{\mathbf{k}'} \frac{1}{\varepsilon - \varepsilon_{n\mathbf{k}'} + i\alpha} &= \frac{V}{N} \int \frac{\rho_n(\varepsilon')}{\varepsilon - \varepsilon' + i\alpha} d\varepsilon' \\ &= \frac{V}{N} \left[ P \int \frac{\rho_n(\varepsilon')}{\varepsilon - \varepsilon'} d\varepsilon' - i\pi \rho_n(\varepsilon) \right]. \end{aligned} \quad (17.6.14)$$

Using the notation

$$F_n(\varepsilon) = P \int \frac{\rho_n(\varepsilon')}{\varepsilon - \varepsilon'} d\varepsilon' \quad (17.6.15)$$

for the principal value,

$$c(\mathbf{R}_0) = \frac{e^{i\mathbf{k} \cdot \mathbf{R}_0}}{1 - V_{nn}(V/N) F_n(\varepsilon) + i\pi V_{nn}(V/N) \rho_n(\varepsilon)}. \quad (17.6.16)$$

The amplitude  $c(\mathbf{R}_0)$  of the wavefunction is large at the impurity for energy values  $\varepsilon_0$  that satisfy

$$1 - V_{nn}(V/N) F_n(\varepsilon_0) = 0. \quad (17.6.17)$$

When this condition is satisfied inside a band, the amplitude remains finite on account of the imaginary part but the  $|c(\mathbf{R}_0)|^2$  vs.  $\varepsilon$  function has a resonance-like maximum. This corresponds to a virtual bound state, as a Lorentzian peak

$$\rho(\varepsilon) = \rho_n(\varepsilon) + \frac{2}{\pi} \frac{\Gamma/2}{(\varepsilon - \varepsilon_0)^2 + (\Gamma/2)^2} \quad (17.6.18)$$

appears in the density of states, where

$$\Gamma/2 = \frac{\pi \rho_n(\varepsilon_0)}{F'(\varepsilon_0)}. \quad (17.6.19)$$

The corresponding density of states is plotted in Fig. 17.11.

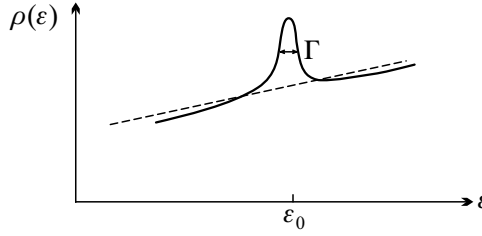


**Fig. 17.11.** The appearance of virtual bound states in the density of states

On the other hand, when the condition (17.6.17) is satisfied outside the band, and thus the imaginary part vanishes, the amplitude of the Wannier function at the impurity becomes infinitely large, indicating a real bound state localized around the impurity. For repulsive potentials ( $V_{nn} > 0$ ) the bound state can appear above the band, at energy  $\varepsilon_0 = \max \varepsilon_{n\mathbf{k}} + \Delta$ , while for attractive potentials ( $V_{nn} < 0$ ) below the band, at energy  $\varepsilon_0 = \min \varepsilon_{n\mathbf{k}} - \Delta$ . The binding energy  $\Delta$  can be determined from the equations

$$1 = \frac{V_{nn}}{N} \sum_{\mathbf{k}} \frac{1}{\Delta + \max \varepsilon_{n\mathbf{k}} - \varepsilon_{n\mathbf{k}}} \quad (17.6.20)$$

and

$$1 = \frac{|V_{nn}|}{N} \sum_{\mathbf{k}} \frac{1}{\Delta + \varepsilon_{n\mathbf{k}} - \min \varepsilon_{n\mathbf{k}}}. \quad (17.6.21)$$

As the dispersion relation is quadratic in the vicinity of the top and bottom of the band, the sum on the right-hand side diverges at  $\Delta = 0$  in one- and two-dimensional systems, thus there exists a bound state with finite binding energy no matter how weak the impurity potential is. In three-dimensional systems bound states exist only for potentials  $V_{nn}$  satisfying either

$$V_{nn} > \left[ \frac{1}{N} \sum_{\mathbf{k}} \frac{1}{\max \varepsilon_{n\mathbf{k}} - \varepsilon_{n\mathbf{k}}} \right]^{-1} \quad (17.6.22)$$

or

$$|V_{nn}| > \left[ \frac{1}{N} \sum_{\mathbf{k}} \frac{1}{\varepsilon_{n\mathbf{k}} - \min \varepsilon_{n\mathbf{k}}} \right]^{-1}. \quad (17.6.23)$$

## Further Reading

1. S. L. Altmann, *Band Theory of Solids, An Introduction from the Point of View of Symmetry*, Clarendon Press, Oxford (1991).
2. H. Jones, *The Theory of Brillouin Zones and Electronic States in Crystals*, 2nd revised edition, North-Holland Publishing Co., Amsterdam (1975).
3. S. Raimes, *The Wave Mechanics of Electrons in Metals*, North-Holland Publishing Company, Amsterdam (1961).



Fundamentals of the Physics of Solids

Volume II: Electronic Properties

Sólyom, J.

2009, XXII, 646 p. 238 illus., Hardcover

ISBN: 978-3-540-85315-2